Theoretical model of ice nucleation induced by acoustic cavitation. Part 1: Pressure and temperature profiles around a single bubble

C. Cogne, S. Labouret, R. Peczalski, Olivier Louisnard, Fabien Baillon, Fabienne Espitalier

Theoretical model of ice nucleation induced by acoustic cavitation. Part 1: Pressure and temperature profiles around a single bubble

C. Cogné [a], S. Labouret [a], R. Peczalski [a,*], O. Louisnard [b], F. Baillon [b], F. Espitalier [b]

[a] University of Lyon, France, Université Claude Bernard Lyon 1, Laboratoire d'Automatique et de Génie des Procédés (LAGEP UMR CNRS 5007), Campus de la Doua, Bât. CPE, 69616 Villeurbanne, France

[b] University of Toulouse, France, Ecole Nationale Supérieure des Mines d'Albi-Carmaux, Centre de Recherche d'Albi en génie des Procédés des Solides Divisés, de l'Énergie et de l'Environnement (RAPSODEE UMR CNRS 5302), Campus Jarlard, 81013 Albi, France

A B S T R A C T

This paper deals with the inertial cavitation of a single gas bubble in a liquid submitted to an ultrasonic wave. The aim was to calculate accurately the pressure and temperature at the bubble wall and in the liquid adjacent to the wall just before and just after the collapse. Two different approaches were proposed for modeling the heat transfer between the ambient liquid and the gas: the simplified approach (A) with liquid acting as perfect heat sink, the rigorous approach (B) with liquid acting as a normal heat conducting medium. The time profiles of the bubble radius, gas temperature, interface temperature and pressure corresponding to the above models were compared and important differences were observed excepted for the bubble size. The exact pressure and temperature distributions in the liquid corresponding to the second model (B) were also presented. These profiles are necessary for the prediction of any physical phenomena occurring around the cavitation bubble, with possible applications to sono-crystallization.

Keywords:
Ultrasound
Cavitation
Single bubble
Heat transfer
Fluid mechanics
Modeling

1. Introduction

1.1. Context and aim of the study

The unstable (inertial) acoustic cavitation of micron size gas bubbles in a liquid medium and especially their violent collapses induce extreme physical conditions (pressures up to tens of GPa, temperatures up to tens of thousands K), inside and in the close vicinity of the bubbles. These conditions are at the origin of spectacular effects like: sonoluminescence, hydroxyl radicals generation, solid surface erosion but also promote the crystallization of solutes in super-saturated solutions or of solvent in super-cooled solutions [1].

In order to keep these phenomena under control, one needs to know exactly the evolution of physical parameters (pressure, temperature, composition) of the gas inside the bubble but also that of the liquid outside as the two are tightly linked one to another.

However, the first concern of most of the studies on acoustic cavitation devoted to interpret sonochemistry and sonoluminescence was the behavior of the gas in the bubble and not that of the surrounding liquid. Thus an approximate way to describe the gas thermal behavior, the heat transfer at the interface and on the liquid side was often adopted in order to obviate the solution of a full set of energy and motion equations in the liquid. In most cases the gas pressure inside the bubble was considered uniform and the motion of the liquid was described by the classical Rayleigh–Plesset equation corrected for liquid compressibility [2–4]. The gas behavior depends strongly on the heat transfer rate across the bubble wall. In a very simplified approach, the slow bubble expansion can be considered as isothermal, while the fast collapse as adiabatic. From that point the basic modeling approach was to describe the gas state by a polytropic equation with a coefficient depending on the Peclet number [5]. As concerns heat transfer in the liquid surrounding the bubble, the simplest assumption was to neglect any thermal gradient and to keep the bubble wall temperature constant at the ambient value [4,6,7]. Another kind of simplified thermal approach was to consider the continuity of the heat flux across the bubble wall and to adopt an arbitrary liquid temperature profile in order to evaluate the heat flux outside the bubble [8,9].

A trend for a more in depth description of the heat transfer between the gas and the liquid was dictated by the recognition of the very important role that plays water vapor in the physics of a collapsing bubble [10–12] and thus the need to take into account the phase change (condensation or evaporation) at the bubble wall and consequently to incorporate a heat balance at the wall in the global model.

* Corresponding author.
E-mail address: peczalski@lagep.univ-lyon1.fr (R. Peczalski).

The first aim of this study was to calculate accurately the pressure and temperature at the bubble wall and in the liquid adjacent to the wall just before and just after the collapse, starting from the mathematical description of the gas behavior and of the bubble wall motion already established and validated in the literature.

The second aim was to show the importance of the assumptions concerning heat transfer at the bubble wall and in the surrounding liquid, by considering two different modeling approaches briefly presented below:

(A) Inside the bubble, a thermal gradient was supposed to exist in the gas over a thin boundary layer near the bubble wall, with a thickness varying accordingly to the wall dynamics. A constant bubble wall (liquid–gas interface) temperature equal to the far field liquid temperature was assumed, with no thermal gradient on the liquid side.
(B) Inside the bubble, the same hypothesis as for case A was adopted. Outside the bubble, a non-linear temperature profile in the liquid was introduced, determined as an approximate analytical solution of the heat conduction–advection equation. Moreover, the wall temperature was evaluated from the heat balance at the wall including water liquid–vapor phase change effect.

1.2. Bibliographical review

In this section a short review of the recent literature concerning the pressure and temperature profiles inside and outside the bubble will be given.

Kwak and Na [8] calculated density, pressure and temperature distributions inside an air bubble by solving analytically the conservation PDEs but neglecting the viscous dissipation and water vapor. The time evolution of the bubble radius was obtained from the Keller–Miksis equation. The heat flux on the liquid side of the bubble wall was expressed by the boundary layer approximation with the layer thickness being a fitting parameter.

Yasui [10] used thoroughly the boundary layer approach in order to evaluate the time profiles of gas temperature, gas pressure, water content and bubble wall temperature for an argon bubble. As concerns the heat transfer between the gas and the liquid, he adopted an arbitrary layer thickness on the gas side and an exponential profile on the liquid side with one fitting parameter and he considered a heat balance at the wall including the phase change effect.

Toegel et al. [6] aimed at determining the amount of water vapor trapped in the bubble during the collapse and its impact on sonoluminescence. They used the boundary layer approach and considered a model consisting of 3 ODEs. The bubble wall radius was evaluated by the Keller–Miksis equation which takes water compressibility into account, the amount of water vapor inside the bubble was derived from a Fickian diffusion flux at the wall, the gas temperature was obtained from an energy balance which takes the heat conduction flux at the bubble wall into account. The mass and heat fluxes on the gas side were calculated using a boundary layer thickness evaluated as diffusion length at a characteristic time scale of the bubble motion. The gas pressure was derived from the van der Waals equation of state. The temperature at the bubble wall was supposed constant and equal to the far liquid one.

Kim et al. [9] solved the rigorous set of PDEs on the gas side but adopted the Keller–Miksis equation for the bubble wall motion and considered a priori a parabolic temperature profile in a thermal boundary layer on the liquid side. The thickness of the liquid boundary layer was estimated by means of an ODE obtained by the integration of the advection–conduction heat transfer equation over the layer. On this basis, the temperature profiles inside and outside an air bubble (without water vapor) were finally determined.

The approach of Vuong et al. [13] was very similar, excepted that no arbitrary temperature profile was adopted on the liquid side. The heat transfer equation in the liquid was transformed by the Plesset–Zwick method and simplified assuming a thin boundary layer (large Peclet's number) in order to obtain finally a linear diffusion equation in Lagrangian boundary layer coordinates which was solved numerically. Vuong et al. [13] used this model to determine the radial gas temperature profiles and bubble wall temperature time profiles for an argon bubble.

Yuan et al. [14] also transformed the advection–conduction equation on the liquid side into a purely diffusive one by means of the Plesset–Zwick variable change but made no further simplification to solve it. He calculated numerically the radial profiles of gas pressure, temperature, velocity and density for a bubble containing only air. The equations of liquid motion were not solved, the Keller–Miksis equation was used to describe the wall dynamics and the liquid compressibility was neglected in the heat transfer equation.

As concerns the heat transfer on the liquid side, Hauke et al. [15] adopted the less restrictive approach as compared to the already cited works. They solved numerically the full set of governing PDE on the gas side and the heat advection–conduction equation on the liquid side (neglecting only the liquid compressibility in the heat transfer equation) using the Keller–Miksis formulation to describe the bubble wall motion. They provided the radial profiles of temperature, pressure and water vapor content inside the bubble as well as the radial temperature profile outside the bubble.

In the context of therapeutic ultrasound, cavitation and bubble dynamics imply very high acoustic pressures and frequencies as well as elevated temperatures. In such conditions, the mass and heat transfer at the bubble wall are particularly important. To address the relevant physics, a reduced-order model of a single, spherical bubble was proposed by Kreider et al. [12] that incorporates phase change at the liquid–gas interface as well as heat and mass transport in both phases. Two approaches for heat transfer on the liquid side were modeled and compared. In the "scaling" approach (SCL model), uniform liquid temperature was assumed everywhere outside of a boundary layer near the bubble wall and a Fickian expression was used for calculating the thermal flux within the boundary layer. A fitting parameter was needed for estimating the boundary layer thickness. In the second approach the Plesset–Zwick analytical solution was used for describing thermal conduction in the presence of advective liquid flow due to bubble wall displacement. The idea of applying the Plesset–Zwick model for heat transfer on the liquid side used in several studies cited above was adopted for this study.

The applied acoustic driving conditions (P_{ac} – acoustic pressure amplitude, f – acoustic frequency, R_0 – initial bubble radius) and the corresponding gas temperature (T_g) as well as gas–liquid interface temperature (T_i) and pressure (P_{li}) at the collapse are presented in Table 1 for the considered publications and compared with the results of this study.

Independently of the conditions considered and thus of the maximal gas temperature obtained in each particular case, all the results shown above can be roughly classified in two groups: a first group where the bubble wall temperature is of the same order of magnitude than the bubble core one [8–10,12] and the second group where the wall temperature is one order of magnitude lower than the core one [13–15]. It is a very marked difference. Furthermore, again in a rough manner, it can be claimed that the results of the first group are based on simplified modeling approaches (boundary layer approximations, arbitrary liquid temperature profiles, analytical solutions) while those of the second group are based on a more comprehensive and rigorous

Table 1
Selected published acoustic cavitation simulations.

Refs.	Gas	P_{ac} (bar)	f (kHz)	R_0 (μm)	T_g (K)	T_i (K)	P_{li} (GPa)
[8]	Air	1.3	26.5	4.5	25,000	17,000	0.8
[10]	Argon and vapor	1.35	20.6	5	10,000	8000	
[14]	Air	1.275	26.4	4.5	15,000	500	4
[13]	Argon	1.3	26.5	4.5	106,000	4000	
[16]	Argon and vapor	1.3	16	5	15,000	293	
[9]	Air	1.33	12.9	5	28,000	13,500	
[15]	Argon and vapor	1.2	22.3	19.3	4300	360	0.13
[12]	Argon	1.2	26.5	4.5		4200	
This study, model A	Air and vapor	1.4	29	5	9300	263	18
This study, model B	Air and vapor	1.4	29	5	11,300	620	23

approaches (spatial variables distributions, no imposed profiles, numerical solutions). The results of the second group should be considered as the reference. It's obvious then that some degree of refinement is needed in order to catch correctly the thermal behavior of the system and this was the start point of our study.

2. Modeling

The exact description of the bubble dynamics during acoustic inertial cavitation can be only achieved by numerical solution of the full set of mass, momentum and energy conservation PDEs on both the gas and liquid side. Nevertheless, it had been proven that mathematically simplified approaches gave satisfactorily precise results [16]. The most straightforward simplification leading to a set of ODEs is the boundary layer approximation where the temperature and species profiles inside the bubble are supposed to be uniform with the exception of a thin boundary layer near the bubble wall [6,12].

In order to keep both mathematical simplicity and physical relevance, the basic concept of our single bubble model is based on Toegel's [6] (see 'Section 1.2') but substantial modifications have been made. First a more realistic representation of the heat transfer at the bubble wall was introduced through an energy balance involving the interfacial phase change heat flux and a conductive heat flux on the liquid side. Second a rigorous thermal and mechanical description was applied to the liquid, with the solution of the heat conduction–advection equation by the Plesset–Zwick [17] method and of the mass and momentum local conservation equations by the Gilmore's [2] method.

In the following subsections, the equations used to describe the acoustic inertial cavitation of a single bubble containing water and air will be presented, with the emphasis on the two approaches adopted in this study for heat transfer at the wall and in the liquid.

2.1. Thermodynamics of the gas

In this study, the focus is on the physics of liquid surrounding the bubble and the goal is to provide reasonably exact liquid pressure and temperature space profiles after the collapse. For this purpose a very fine model for the gas in the bubble is not necessary and thus global balances and state equations were used on the inner side of the bubble. The gas pressure P_g was considered uniform and evaluated by the classical equation of state with the van der Waals's correction for an incompressible (hard) core:

$$P_g = \frac{(N_v + N_a)\Re T_g}{\frac{4\pi}{3}(R^3 - R_{hc}^3)} \tag{1}$$

where N_a is the number of air moles, N_v the number of water vapor moles within the bubble, R the bubble radius, R_{hc} the hard core radius and T_g the gas temperature. While N_a was considered constant, N_v was considered to vary due to vapor diffusion through the air in the bubble from or to the wall. The vapor quantity balance in the bubble was based on a Fickian expression and a boundary layer assumption:

$$\frac{dN_v}{dt} = \frac{3D_{va}}{R\delta_{mg}}\left(\frac{4\pi R^3 P_{vsat}(T_i)}{3\Re T_i} - N_v\right) \tag{2}$$

where D_{va} is the water vapor in dry air diffusivity and P_{vsat} is the saturated water vapor pressure. The gas temperature T_g was considered uniform except in the close vicinity of the bubble wall and obtained from an overall bubble energy balance where the heat flux at the wall was evaluated by the boundary layer approximation:

$$(C_{vv}N_v + C_{va}N_a)\frac{dT_g}{dt} = -P_g 4\pi R^2 \frac{dR}{dt} + \lambda_g 4\pi R^2 \frac{T_g - T_i}{\delta_{tg}} + \frac{dN_v}{dt} \times (C_{pv}T_i - C_{vv}T_g) \tag{3}$$

where C_v or C_p are specific heat capacities for constant volume or constant pressure and T_i is the time dependent temperature at the bubble wall which must be obtained like a part of the solution of the global bubble cavitation model.

The boundary layer thicknesses for mass (δ_{mg}) and heat (δ_{tg}) transfer at the bubble wall were evaluated as a diffusion length during the characteristic time scale of the bubble oscillation:

$$\delta_{mg} = \min\left(\sqrt{D_{va}\frac{R}{|\dot{R}|}}, \frac{R}{2}\right) \tag{4}$$

$$\delta_{tg} = \min\left(\sqrt{\alpha_g\frac{R}{|\dot{R}|}}, \frac{R}{2}\right) \tag{5}$$

The pressure and temperature correlations for gas properties involved in the above equations: water vapor mass diffusivity in air D_{va}, vapor–air mixture heat conductivity λ_g, vapor–air mixture heat diffusivity α_g, saturated vapor pressure P_{vsat}, heat capacities C_{vv}, C_{va} C_{pv}, were all extracted from the well-known compilation of Poling et al. [18].

2.2. Mechanics of the wall and of the liquid

A single spherical gas bubble surrounded by liquid water is considered. The radial coordinate r originates at the center of the bubble. The mass and momentum conservation equations (Navier–Stokes equations) for a spherically symmetric liquid flow write respectively:

$$\frac{\partial \rho_l}{\partial t} + \frac{\partial}{\partial r}(\rho_l u_l) + \frac{2\rho_l u_l}{r} = 0 \tag{6}$$

$$\frac{\partial u_l}{\partial t} + u_l\frac{\partial u_l}{\partial r} + \frac{1}{\rho_l}\frac{\partial P_l}{\partial r} = 0 \tag{7}$$

where u_l is the liquid velocity, P_l is the liquid pressure and ρ_l its density. The boundary conditions associated to these equations are the liquid pressures and velocities at the wall and far away from the wall:

– at the bubble wall (underscript i) the velocity is determined by the wall motion, the pressure can be expressed by considering the mechanical forces balance involving the pressure force exerted by the gas, the surface tension force and the viscous friction force:

$$u_{li} = U = \frac{dR}{dt} \tag{8}$$

$$P_{li} = P_g - \frac{2\sigma_{gl}}{R} - \frac{4\mu_l}{R}\frac{dR}{dt} \tag{9}$$

where σ_{gl} is the gas–liquid surface tension and μ_l is the liquid dynamic viscosity;

– in the liquid far away from the bubble (underscript ∞), the velocity vanishes and the pressure is the sum of the ambient pressure and the driving acoustic pressure:

$$u_{l\infty} = 0 \tag{10}$$

$$P_{l\infty} = P_0 - P_{ac}\sin(\omega t) \tag{11}$$

As first demonstrated by Gilmore [2], these PDEs governing liquid mechanics around a spherical bubble can be reduced to a set of ODEs by using the Kirkwood–Bethe hypothesis. This hypothesis states that the quantity denoted here by z:

$$z = r\left(h_l + \frac{u_l^2}{2}\right) \tag{12}$$

is constant along any path traced by a point moving outward from the bubble wall with a varying total velocity which is a sum of the sound velocity in the liquid and of the liquid velocity ($c_l + u_l$). Such a path is called a characteristic and the position of the point is described by:

$$\frac{dr}{dt} = c_l + u_l \tag{13}$$

According to the above equations, differentiation along the characteristic gives:

$$\frac{dz}{dr} = \left(\frac{\partial}{\partial r} + \frac{1}{c_l + u_l}\frac{\partial}{\partial t}\right)z = 0 \tag{14}$$

In order to introduce the liquid sound velocity and the liquid enthalpy the following definitions are used:

$$c_l^2 = \frac{dP_l}{d\rho_l} \tag{15}$$

$$dh_l = \frac{dP_l}{\rho_l} \tag{16}$$

After combining the above definitions and the liquid state equation (Tait's equation, see below) with the starting mass and momentum conservation equations, the velocity and the pressure in the liquid are finally described as follows:

$$\frac{du_l}{dt} = \frac{1}{c_l - u_l}\left(-\frac{2c_l^2 u_l}{r} + \frac{(c_l + u_l)}{r^2}Z\right) \tag{17}$$

$$\frac{dP_l}{dt} = \frac{1}{c_l - u_l}(m(P_l + \beta)^{1/m})\ \ \frac{4c_l^2 u_l^2}{r} - \frac{(c_l + u_l)^2}{r^2}Z\Bigg) \tag{18}$$

where Z is the z value evaluated at the bubble wall and then:

$$Z = R\ \ H_l + \frac{1}{2}\frac{dR^2}{dt}\Bigg) \tag{19}$$

Following the same mathematical lines, the bubble wall motion is written as:

$$R\frac{dU}{dt}\left(1 - \frac{U}{C_l}\right) + \frac{3}{2}U^2\left(1 - \frac{U}{3C_l}\right) = H_l\left(1 + \frac{U}{C_l}\right) + \frac{R}{C_l}U\frac{dH_l}{dR}\left(1 - \frac{U}{C_l}\right) \tag{20}$$

$$\frac{dR}{dt} = U \tag{21}$$

where U is the bubble wall velocity, H_l and C_l are respectively the liquid enthalpy and sound velocity at the bubble wall.

Using the Tait's form of state equation for liquid which writes:

$$\rho_l(P,T) = \rho_{l0}(T)\left(\frac{P_l + \beta}{P_{l0} + \beta}\right)^{1/m} = \frac{\rho_0}{[1 + c(T - T_0)^d]}\left(\frac{P_l + \beta}{P_{l0} + \beta}\right)^{1/m} \tag{22}$$

the enthalpy and the sound velocity can be evaluated everywhere in the liquid (and specifically at the bubble wall) as a function of pressure by the following expressions:

$$h_l = \int_{P_{l\infty}}^{P_l}\frac{dP_l}{\rho_l} = \frac{m}{m-1}\frac{(P_{l0} + \beta)^{\frac{1}{m}}}{\rho_{l0}(T)}[(P_l + \beta)^{\frac{m-1}{m}} - (P_{l\infty} + \beta)^{\frac{m-1}{m}}] \tag{23}$$

$$c_l = \left(\frac{dP_l}{d\rho_l}\right)^{\frac{1}{2}} = \left(\frac{m(P_{l0} + \beta)}{\rho_{l0}(T)}\right)^{\frac{1}{2}}\left(\frac{P_l + \beta}{P_{l0} + \beta}\right)^{\frac{m-1}{2m}} \tag{24}$$

The coefficients of the Tait's equation for the low pressure domain were directly read from the study of Ridah [19] and are given in Table 2. The coefficients for the high pressure domain were obtained by fitting the Tait's equation to the data compiled by Choukroun and Grasset [20]. The density correction for temperature (function $\rho_{l0}(T)$) was adopted from the same study (see Table 2). The water gas–liquid interfacial energy σ_{gl} and the liquid water dynamic viscosity μ_l were also correlated to pressure and temperature [21–23]. It is worth noting that even in case of studies proposing complex models, published simulations were mostly realized with constant fluid properties, especially concerning the liquid. One of the advantages of the present study is that the gas and liquid properties are systematically correlated to pressure and temperature, even for very high pressures (as far as data exist).

2.3. Heat transfer at the wall and in the liquid

2.3.1. Model A

The heat flux between the gas bubble and the ambient liquid must be known for a proper evaluation of the bubble thermodynamics, motion and chemistry. For this purpose, according to the equations presented above, the fundamental issue is the evaluation of the bubble wall (or gas–liquid interface) temperature. The question arises if there is a simple way of estimating this temperature near the collapse. At this special moment, the variation of the gas temperature is very rapid and the hypothetical thermal boundary layer very narrow. Thus, in a first attempt one can consider the classical case of two semi-infinite solid bodies at different initial temperatures which are bring into contact. The heat conduction textbook's solution of this problem states that the ratio of temperature differences between the far and interface temperature for each of the two bodies corresponds to the square root of the ratio of their thermal effusivities (the effusivity is the product of density, thermal conductivity and specific heat capacity). For standard

Table 2
Coefficients of the state equation for liquid water (ρ: kg/m^{-3}, T: K, P: MPa).

	ρ_0	T_0	P_0	c	d	β	m
$P < 1000$	1007	180	0.1013	2.963×10^{-9}	3.17	303.9	7
$P > 1000$	Same as above					80	12.5

values of thermophysical properties of liquid water and air, the temperature gradient at the liquid side will be 2 or 3 order of magnitude smaller than the one at the gas side and so the interface temperature should be very close to the far liquid temperature. This estimation may justify the assumption of constant interface temperature used by several authors (see 'Section 1') for acoustic cavitation modeling. Such an assumption was adopted also for the simplest thermal model considered in this study (model A). It writes simply: $T_i = T_{1\infty} = \text{constant}$.

In this model, the bubble wall temperature is maintained at its lowest possible level and thus the cooling effect of the liquid is maximal.

2.3.2. Model B

The approach presented above is not really satisfactory because during the collapse the gas thermodynamical state is very far away from the standard one, the huge bubble volume reduction resulting in an enormous gas density increase and consequently thermal effusivity increase. The gas effusivity can be expected to become comparable to the liquid one at the collapse and the interface temperature to shift toward to the core gas temperature. Moreover, a vapor–liquid phase change takes place at the bubble wall and a heat balance equation involving the energy sink (or release) due to water evaporation (or condensation) is needed. A more rigorous approach accounting for these effects and also for the bubble dynamics is proposed below.

According to the mechanics of inertial cavitation (see preceding section), the bubble radius R is a given function of time. Due to the radial movement of the bubble wall the liquid is displaced in the vicinity of the bubble. The heat transfer equation for incompressible liquid with constant thermal properties involving molecular diffusion and advection due to liquid motion is written as:

$$\frac{\partial T_l}{\partial t} + u_l \frac{\partial T_l}{\partial r} = \frac{\alpha_l}{r^2} \frac{\partial}{\partial r}\left(r^2 \frac{\partial T_l}{\partial r}\right) \tag{25}$$

where the heat diffusivity is defined as $\alpha_l = \lambda_l/(\rho_l c_{pl})$ and the liquid velocity for incompressible flow is given by:

$$u_l = \frac{R^2}{r^2}\frac{dR}{dt} \tag{26}$$

For the determination of the temperature profile, the liquid incompressibility is assumed, but for determination of the pressure profile the compressibility of liquid has been accounted for as explained in preceding subsection.

The initial and boundary conditions for the above equation are given by:

– boundary condition at the bubble wall: $r = R(t)$

$$-\lambda_l \frac{\partial T_l}{\partial r} = \frac{\Phi_{li}(t)}{4\pi R^2(t)} \tag{27}$$

– boundary condition in far liquid: $r = \infty$

$$T_l = T_{l\infty} \tag{28}$$

– initial condition: $t = 0$

$T_l = T_{l\infty}$

The time dependent heat flux at the bubble wall Φ_{li} corresponds to the conductive heat flux in the gas inside the bubble and the latent heat flux of water evaporation/condensation at the wall:

$$\Phi_{li}(t) = 4\pi R(t)^2 \lambda_g \frac{T_g(t) - T_i(t)}{\delta_{tg}(t)} - \frac{dN_v}{dt} M_v \Delta h_{vap}(T_i) \tag{29}$$

In order to solve analytically this problem, independent variable changes will be operated according to the Plesset–Zwick method (see 'Section 1.2').

First, the spatial variable r will be replaced by a new variable y defined by:

$$y = \frac{r^3 - R^3(t)}{3} \tag{30}$$

The new variable corresponds dimensionally to a volume of liquid and (if liquid incompressibility is assumed) is associated to a material point moving along with the displacement of the bubble wall. The new variable is thus a Lagrangian one and the transfer equation will lose its advective term and will become a strictly diffusive one:

$$\frac{\partial T_l}{\partial t} = \alpha_l \frac{\partial}{\partial y}\left[\left(3y + R^3(t)\right)^{4/3} \frac{\partial T_l}{\partial y}\right] \tag{31}$$

In the limit $y \ll R^3$, what means that the temperature in the liquid is supposed to vary significantly only in a small distance from the bubble wall, the above equation becomes:

$$\frac{1}{R^4(t)} \frac{\partial T_l}{\partial t} = \alpha_l \frac{\partial^2 T_l}{\partial y^2} \tag{32}$$

Now using a new temporal variable τ defined by

$$\tau = \int_0^t R^4(t)dt \tag{33}$$

the heat transfer equation transforms simply to:

$$\frac{\partial T_l}{\partial \tau} = \alpha_l \frac{\partial^2 T_l}{\partial y^2} \tag{34}$$

what is a canonical parabolic PDE which solution obtained by the Laplace transform can be found in the references cited above but also in heat conduction textbooks. This solution, for a prescribed time dependent heat flux Φ_{li} at the boundary, writes:

$$T_l(y,\tau) - T_{l\infty} = \frac{\sqrt{\alpha_l}}{4\pi^{3/2}\lambda_l} \int_0^\tau \frac{\Phi_{li}(x)}{R^4(x)\sqrt{\tau - x}} \times \exp\left(-\frac{y^2}{4\alpha_l(\tau - x)}\right) dx \tag{35}$$

The above approach based on the Plesset–Zwick approximation was adopted for the final thermal model of this study (model B). The literature expressions of heat conductivity λ_l [24] and specific heat capacity c_{pl} [20] as function of temperature were used. The influence of pressure on these two parameters was neglected.

The model is very sensitive to mass diffusivity (D_{va}) and heat diffusivities on the gas side (α_g) and on the liquid side (α_l). As concerns the bubble interior, the gas thermal properties are rather well known and well correlated to pressure and temperature [18]. Moreover, the boundary layer approach inside the bubble was proven to give satisfactory results compared to a full solution considering a radial temperature profile inside the bubble [16]. However, the boundary layer approximation outside the bubble suffers from a lack of generally accepted time scale definition for the diffusion length evaluation and from a lack of reliable liquid thermal data, especially for high pressures. In the frame of this study, a boundary layer approach for heat diffusion on the liquid side was tried applying the same time scale as on the gas side (see Eqs. (4) and (5)). That resulted in a not realistic very high temperature at the bubble wall (around 1700 K) at the moment of the collapse and this approach was abandoned. Kwak and Na [8], Yasui [10] and Kreider et al. [12] have used an arbitrary temperature profile or a boundary layer thickness with a fitting parameter. The

Plesset–Zwick approximation [12–14] adopted here avoids introducing such a kind of workarounds.

2.4. Numerical solution of the problem

The bubble dynamics was simulated by solving simultaneously the Eqs. (2), (3), (20) and (21) as a system of first order ODEs by means of MATLAB routine ODE113. At any time t, the solution provided the bubble radius R, bubble wall velocity U, the gas temperature inside the bubble T_g and the vapor quantity inside the bubble N_v. The gas pressure P_g inside the bubble was then calculated by Eq. (1) and the liquid temperature T_i at the bubble wall by Eq. (35). This last equation provided also the liquid temperature distribution all around the bubble.

The liquid dynamics around the bubble was simulated by solving simultaneously the Eqs. (13), (17) and (18) as a system of first order ODEs (MATLAB routine ODE45). The calculations were carried out along a characteristic, each characteristic originating at the bubble wall. Starting from the given conditions at the bubble wall (R, H_l, C_l), for any time subsequent time t, the solution provided the corresponding radial position r along the characteristic and the value of the liquid pressure P_l and liquid temperature T_l at this position. Many characteristics had to be used in order to cover the entire geometrical domain around the bubble.

3. Results and discussion

3.1. Pressure and temperature at the bubble wall

In this section the simulations obtained with the two thermal models (A and B) will be compared. The temporal evolutions of the bubble wall position, the internal gas temperature, the liquid temperature and pressure at the bubble wall are presented on Figs. 1–3. The Figs. 2 and 3 are focused on the first collapse. The gas pressure inside the bubble and the liquid pressure at the bubble wall were found to be quite identical at the collapse and only the liquid pressure was shown. The acoustic and ambient conditions used for the calculations are given in Table 3. The ambient temperature is below zero because this model was intended to be applied later to the case of water freezing induced by ultrasound.

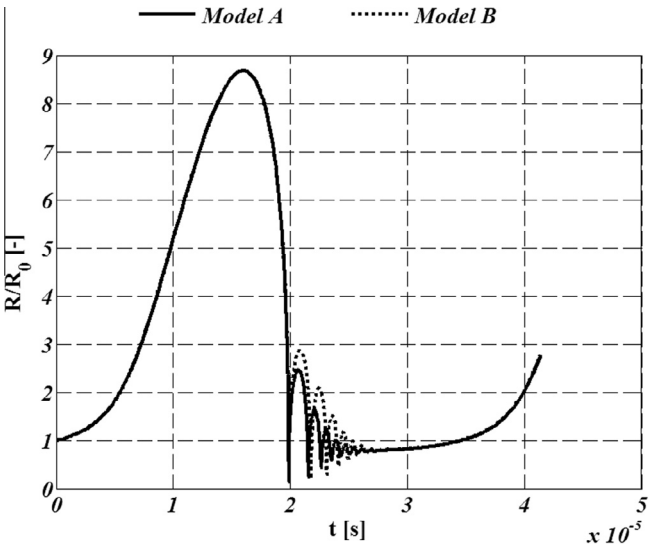

Fig. 1. The time profiles of the bubble radius (R) over one period of the acoustic excitation.

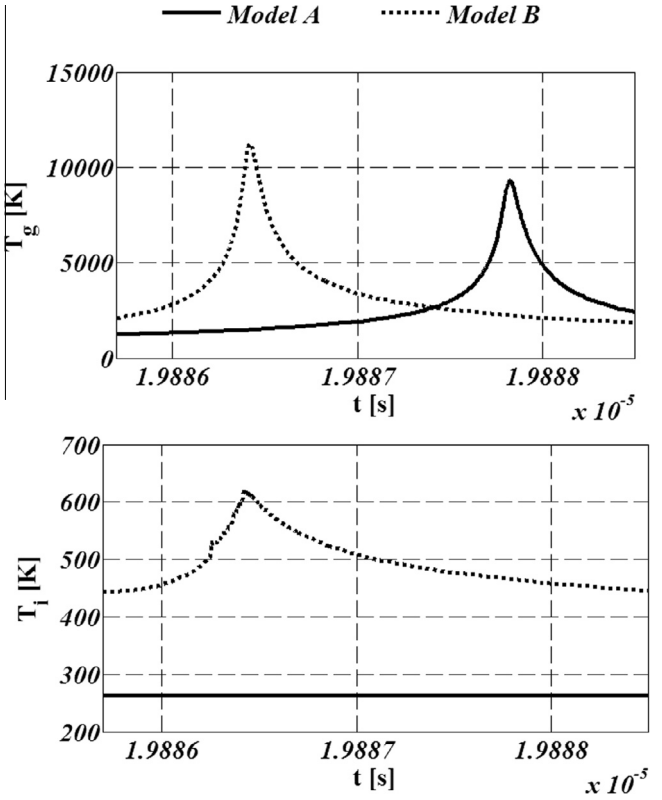

Fig. 2. The time profiles of the internal gas temperature (T_g) and the interfacial liquid temperature (T_i) at the collapse.

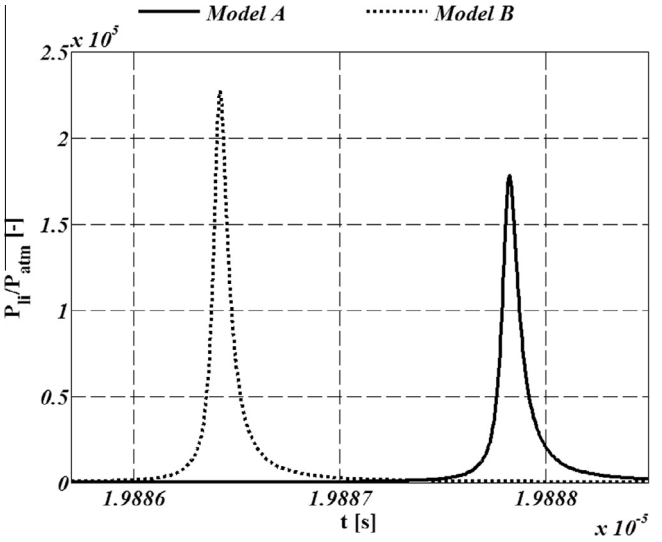

Fig. 3. The time profiles of the interfacial liquid pressure (P_{li}) at the collapse.

Table 3
Parameters of the simulations.

R_0 (μm)	$T_{l\infty}$ (°C)	P_{ac} (bar)	f (kHz)
5	−10	1.4	29

As reported elsewhere, during inertial cavitation the bubble expands rather slowly to several times its initial size and then collapses violently. The huge nearly adiabatic compression of the gas due to the collapse heats up very strongly the bubble core

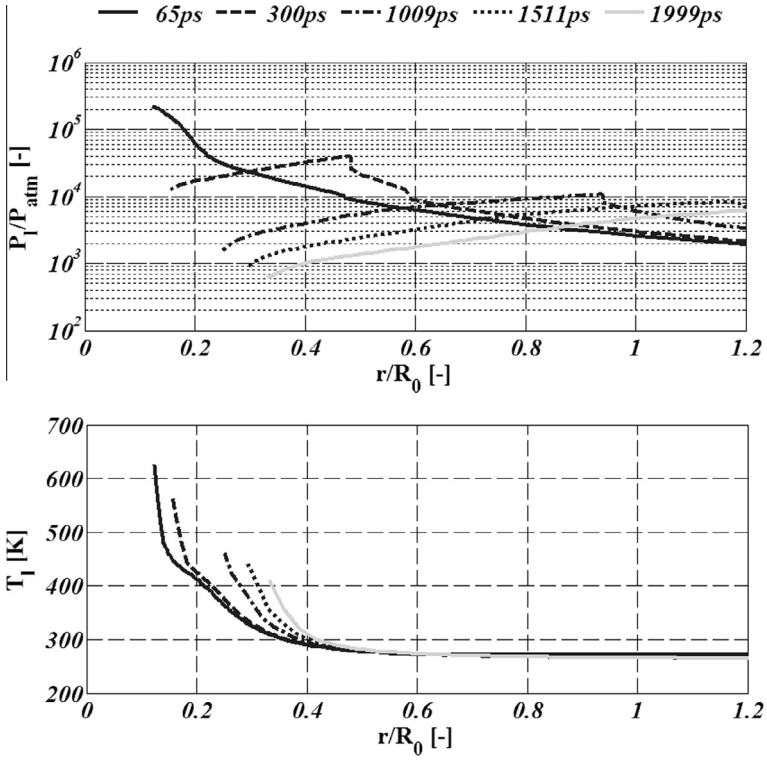

Fig. 4. The radial profiles of liquid pressure (P_l) and liquid temperature (T_l) around a bubble for different times after the collapse.

inducing a temperature and pressure peaks. According to Fig. 1, the thermal model did not affect sensibly the dynamic behavior of the bubble wall, excepted for the post-collapse rebounds. However, the thermal model affected considerably all the thermodynamic variables inside the bubble and at the wall. The temperature of the gas inside the bubble was found to be 20% lower for the model A (9300 K) than for model B (11,300 K). This can be justified by the fact that model A corresponded to a stronger cooling rate of the bubble (see Fig. 2). Consequently, the pressure of liquid at the wall (nearly equal to the internal gas pressure at the collapse) was also 20% lower for case A (18 GPa) than for case B (23 GPa) as shown on Fig. 3. The time of the collapse was slightly different for the two cases.

The thermal model had by evidence the strongest impact on the temperature at the bubble wall. According to Fig. 2, this interfacial temperature for comprehensive model B was rather moderate (620 K) and did not reach the critical value for water (647 K). It was much closer to the far liquid (ambient) temperature (263 K) than to the core temperature (11,300 K). However, substituting the interfacial temperature by the ambient temperature appears clearly as a not realistic hypothesis, especially if temperature sensitive physical and chemical phenomena in the liquid are studied. This result corroborates those corresponding to the most elaborate models and numerical simulations published in the literature (see Table 1), with some caution because of different parameters (acoustic frequency, gas specie).

The bubble interior energy balance (Eq. (3)) does not include the heat effect of chemical reactions. However, the water vapor trapped within the bubble undergoes rapid reactions when the temperature exceeds 3000 K and leads to the production of hydroxyl radicals. Several authors included chemical reactions in their cavitation model and concluded that the endothermic dissociation of water vapor significantly reduced the bubble core peak temperatures (T_g) achieved at the collapse. According to Hauke et al. [15] (argon and vapor, P_{ac} = 1.2 bar, f = 22.3 kHz, R_0 = 19.3 μm) vapor dissociation accounts for 10% of the core temperature (T_g) reduction and according to Storey and Szeri [25] (argon plus vapor, P_{ac} = 1.2 bar, f = 26.5 kHz, R_0 = 4.5 μm), it accounts for up to 30%. But the liquid temperature (T_i) at the bubble wall was supposed and shown to be much less impacted. Supplementary simulations with our model B showed that a 30% decrease of T_g corresponded to a 5% decrease in T_i. So the error of calculating T_i due to chemical reactions omission would be no more than 5%, which is in the range, or even below, of the error induced by the uncertainty on gas and liquid thermo-physical properties.

The model B proposed in this study comprehends all the relevant thermal phenomena and at the same time it writes mathematically rather simply. The thermal model B coupled with the fluidics and thermodynamics model of cavitation proposed in this study writes as a set of ODE's and solves more conveniently (MATLAB) and quickly than a full multi-physics model based on PDE's which requires a finite element software. At the same time, this model gives realistic results, similar to those provided by complex models and sophisticated solvers. It could be a useful tool for fast prediction of pressure and temperature conditions around a single cavitating bubble, with applications to sono-chemistry and sono-crystallization. In the next part of this paper, only simulations obtained with model B will be presented.

3.2. Liquid pressure and temperature near the bubble

The spatial distributions of the temperature and pressure in the liquid outside the bubble just after the collapse are presented on Fig. 4. The first considered time (65 ps) corresponds to the time of maximum pressure at the bubble wall, the time zero being the time of the collapse defined as the maximum of bubble wall velocity.

As observed on liquid pressure profiles, a pressure peak which can be assimilated to a shockwave propagates in the liquid at a very high speed and is attenuated as moving away from the

bubble. As concerns liquid temperature, the spatial profiles present 2 different zones: a very narrow (100–200 nm) zone with a very steep quasi-linear gradient and a broader (1–2 μm) zone with a progressively decreasing gradient. The occurrence of these two zones and the important spatial extension of the second one invalidates a simple calculation of the heat flux in the liquid based on a linear temperature profile over a thermal boundary layer and proves well the necessity of a very fine description of heat transfer between the bubble and the liquid.

Besides, according to Fig. 4, the zone of strong temperature variation was roughly two times smaller than the zone of very high pressures (above 1 GPa). That means that an area with already nearly ambient temperature but still very high pressure existed near the bubble after the collapse. This conjunction could promote sono-crystallization processes, in solutions [26] or melts [7].

4. Conclusion

On the ground of a literature review, a mathematically simple but physically comprehensive model of inertial acoustic cavitation and especially of a single gas bubble collapse was developed. Two different approaches were proposed for modeling the heat transfer between the ambient liquid and the gas: the simplified approach (A) with liquid acting as perfect heat sink, the rigorous approach (B) with liquid acting as a normal heat conducting medium. The values of the bubble radius, gas temperature, interface temperature and pressure corresponding to the above models were calculated in a time interval encompassing the collapse and compared. Important differences were observed for gas and liquid temperatures and may be interpreted as a rebuttal against the simplified heat transfer description, often used in cavitation models. The exact pressure and temperature distributions in the liquid after the collapse, calculated with the second model (B), were presented. The temperature at the bubble wall was found much closer to the ambient liquid one than to the bubble core one. An area with already nearly ambient temperature but still very high pressure was observed near the bubble just after the collapse. These results are the basis for the prediction of any physical phenomena occurring around the bubble, especially of the dissolved or melted phase crystallization, and thus the basis for the control of industrial processes relying on acoustic cavitation. An application to ice sono-crystallization in aqueous solutions will be described in the second part of this paper.

Acknowledgment

This work was financially supported by the French governmental research funding agency ANR in the frame of the project '09-BLAN-0040-SONONUCLICE'.

References

[1] F. Baillon, F. Espitalier, C. Cogné, R. Peczalski, O. Louisnard, Crystallization and Freezing Processes Assisted by Power Ultrasound, in: Juan A. Gallego-Juárez, Karl Graff (Eds.), Power Ultrasonics: Applications of High-Intensity Ultrasound, first ed., Woodhead Publishing, Cambridge, 2014.
[2] F.R. Gilmore, The growth or collapse of a spherical bubble in a viscous compressible liquid, California Institute of Technology Pasadena (Technical Report, unpublished), 1952.
[3] J.B. Keller, M. Miksis, Bubble oscillations of large amplitude, J. Acoust. Soc. Am. 68 (2) (1980) 628–633.
[4] A. Prosperetti, Y. Hao, Modelling of spherical gas bubble oscillations and sonoluminescence, Philos. Trans. R. Soc. London 357 (1999) 203–223.
[5] M.S. Plesset, A. Prosperetti, Bubble dynamics and cavitation, Ann. Rev. Fluid Mech. 9 (1977) 145–185.
[6] R. Toegel, B. Gompf, R. Pech, Does water vapor prevent upscaling sonoluminescence?, Phys Rev. Lett. 85 (15) (2000) 3165–3168.
[7] M. Saclier, R. Peczalski, J. Andrieu, A theoretical model for ice primary nucleation induced by acoustic cavitation, Ultrason. Sonochem. 17 (2010) 98–105.
[8] H. Kwak, J. Na, Hydrodynamic solutions for a sonoluminescing gas bubble, Phys. Rev. Lett. 77 (1996) 4454–4457.
[9] K. Kim, B. Byun, H. Kwak, Temperature and pressure fields due to collapsing bubble under ultrasound, Chem. Eng. J. 132 (2007) 125–135.
[10] K. Yasui, Alternative model of single-bubble sonoluminescence, Phys. Rev. 56 (6) (1997) 6750–6760.
[11] A.J. Szeri, B.D. Storey, A. Pearson, J.R. Blake, Heat and mass transfer during the violent collapse of nonspherical bubbles, Phys. Fluids 15 (2003) 2576–2586.
[12] W. Kreider, L.A. Crum, M.R. Bailey, O.A. Sapozhnikov, A reduced-order, single-bubble cavitation model with applications to therapeutic ultrasound, J. Acoust. Soc. Am. 130 (5) (2011) 3511–3530.
[13] V.Q. Vuong, A.J. Szeri, D.A. Young, Shock formation within sonoluminescence bubbles, Phys. Fluids 11 (1) (1999) 10–17.
[14] L. Yuan, H.Y. Cheng, M.C. Chu, P.T. Leung, Physical parameters affecting sonoluminescence. A self-consistent hydrodynamic study, Phys. Rev. 57 (4) (1998) 4265–4280.
[15] G. Hauke, D. Fuster, C. Dopazo, Dynamics of a single cavitating and reacting bubble, Phys. Rev. E 75 (2007) 1–14.
[16] B.D. Storey, A.J. Szeri, A reduced model of cavitation physics for use in sonochemistry, Proc. R. Soc. A Math. Phys. Eng. Sci. 457 (2001) 1685–1700.
[17] M.S. Plesset, S.A. Zwick, A nonsteady heat diffusion problem with spherical symmetry, J. Appl. Phys. 23 (1) (1952) 95–98.
[18] B.E. Poling, J.M. Prausnitz, J.P. O'Connell, The properties of gases and liquids, fifth ed., McGraw-Hill, New York, 2001.
[19] S. Ridah, Shock waves in water, J. Appl. Phys. 64 (1986) 152–158.
[20] M. Choukroun, O. Grasset, Thermodynamic model for water and high-pressure ices up to 2.2 GPa and down to the metastable domain, J. Chem. Phys. 127 (2007) 124506.
[21] E. Mezger, Loi de variation de la tension superficielle avec la température, Journal de physique 10 (1946) 303–309.
[22] M.L. Huber, R.A. Perkins, A. Laesecke, D.G. Friend, J.V. Sengers, M.J. Assael, I.N. Metaxa, E. Vogel, R. Mares, K. Miyagawa, New international formulation for the viscosity of H20, J. Phys. Chem. Ref. Data 38 (2) (2009) 101–125.
[23] E.H. Abramson, Viscosity of water measured to pressure of 6 GPa and temperatures of 300 °C, Phys. Rev. E 76 (2007) 051203.
[24] M.L.V. Ramires, C.A. Nieto de Castro, Y. Nagasaka, A. Nagashima, M.J. Assael, W.A. Wakeham, Standard reference data for the thermal conductivity of water, J. Phys. Chem. Ref. Data 24 (1995) 1377–1381.
[25] B.D. Storey, A.J. Szeri, Water vapour, sonoluminescence and sonochemistry, Proc. R. Soc. London A Math. Phys. Eng. Sci. 456 (2000) 1685–1709.
[26] C. Virone, H.J.M. Kramer, G.M. van Rosmalen, A.H. Stoop, T.W. Bakker, Primary nucleation induced by ultrasonic cavitation, J. Cryst. Growth 294 (1) (2006) 9–15.